Autophosphorylation is sufficient to release Mps1 kinase from native kinetochores

Lori B. Koch[a,b,1], Kwaku N. Opoku[b,c,1], Yi Deng[c], Adrienne Barber[a], Aimee J. Littleton[a], Nitobe London[a,b], Sue Biggins[a,2], and Charles L. Asbury[c,2]

[a]Howard Hughes Medical Institute, Division of Basic Sciences, Fred Hutchinson Cancer Research Center, Seattle, WA 98109; [b]Molecular and Cellular Biology Program, University of Washington, Seattle, WA 98195; and [c]Department of Physiology and Biophysics, University of Washington, Seattle, WA 98195

Edited by Andrew W. Murray, Harvard University, Cambridge, MA, and approved July 22, 2019 (received for review January 30, 2019)

Accurate mitosis depends on a surveillance system called the spindle assembly checkpoint. This checkpoint acts at kinetochores, which attach chromosomes to the dynamic tips of spindle microtubules. When a kinetochore is unattached or improperly attached, the protein kinase Mps1 phosphorylates kinetochore components, catalyzing the generation of a diffusible "wait" signal that delays anaphase and gives the cell time to correct the error. When a kinetochore becomes properly attached, its checkpoint signal is silenced to allow progression into anaphase. Recently, microtubules were found to compete directly against recombinant human Mps1 fragments for binding to the major microtubule-binding kinetochore element Ndc80c, suggesting a direct competition model for silencing the checkpoint signal at properly attached kinetochores. Here, by developing single-particle fluorescence-based assays, we tested whether such direct competition occurs in the context of native kinetochores isolated from yeast. Mps1 levels were not reduced on kinetochore particles bound laterally to the sides of microtubules or on particles tracking processively with disassembling tips. Instead, we found that Mps1 kinase activity was sufficient to promote its release from the isolated kinetochores. Mps1 autophosphorylation, rather than phosphorylation of other kinetochore components, was responsible for this dissociation. Our findings suggest that checkpoint silencing in yeast does not arise from a direct competition between Mps1 and microtubules, and that phosphoregulation of Mps1 may be a critical aspect of the silencing mechanism.

mitosis | spindle assembly checkpoint | single molecule fluorescence

Accurate segregation of chromosomes into daughter cells is essential for the development and survival of all organisms. However, the process is prone to errors that must be detected and corrected to avoid chromosome missegregation events that would generate aneuploidy, a hallmark of cancer and other diseases (reviewed in ref. 1). A surveillance system called the spindle assembly checkpoint prevents errors by delaying segregation until every chromosome has made proper bioriented attachments to microtubules from opposite poles (reviewed in refs. 2 and 3). Checkpoint signaling is initiated by recruitment of a hierarchy of proteins to the kinetochore, which subsequently generate a diffusible inhibitory signal that delays anaphase. While the activation of this "wait" signal has been extensively characterized, the events that trigger its deactivation remain unclear. Both premature and abnormally late deactivation of the spindle assembly checkpoint can lead to genetic abnormalities associated with cancer (4, 5), so understanding its mechanism is relevant to human health.

The conserved protein kinase Mps1 is the most upstream component of the spindle assembly checkpoint signaling cascade, and it also regulates sister kinetochore biorientation through an independent mechanism (reviewed in ref. 6). Mps1 expression varies in a cell cycle-dependent manner, with protein levels peaking during prometaphase and then declining during anaphase (7, 8). Mps1 localizes to kinetochores by associating with the microtubule-binding protein Ndc80 (9–11), an ideal position for sensing and responding to the attachment status of the kinetochore. Mps1 kinetochore localization is highly dynamic, cycling on and off the kinetochore with a half-life of several seconds in mammalian cells (12, 13). Stable tethering of Mps1 to the central kinetochore causes constitutive activation of the spindle assembly checkpoint, suggesting that regulation of the Mps1 kinetochore localization is critical for proper checkpoint silencing (13–15). In addition, the levels of Mps1 on kinetochores are highest in prometaphase when attachments are being established, and they decline as bioriented attachments are achieved at metaphase (12, 14, 16). Thus, the release of Mps1 protein from kinetochores appears to be important for silencing the checkpoint.

A simple and elegant model for spindle assembly checkpoint silencing posits that Mps1 and microtubules compete directly for binding to Ndc80, thereby linking microtubule attachment to the release of Mps1 and deactivation of checkpoint signaling (17, 18). Although this direct competition model is supported by biochemical data collected using recombinant human protein fragments, it does not account for a residual pool of Mps1 that remains on bioriented metaphase kinetochores in cells (12, 14, 17). In addition, there is evidence for other mechanisms, such as spatial or enzymatic regulation of Mps1, which might account for the loss of Mps1 checkpoint activity on biorientation (13, 14, 19–24). Despite the evidence for multiple mechanisms controlling Mps1 localization and checkpoint activity, it has been difficult to discern their relative importance or sequential order, given the intertwined nature of these events within cells. Thus, the mechanisms that cause Mps1

Significance

Chromosomes carry our genetic material and must be precisely copied and partitioned into daughter cells during cell division. To ensure correct partitioning, a signaling cascade called the spindle assembly checkpoint delays cell division until all chromosomes are correctly attached to microtubules, the dynamic filaments that drive chromosome movements. If even a single chromosome is unattached or incorrectly attached, an enzyme, Mps1, initiates checkpoint signaling by binding to and modifying kinetochores, the large protein complexes that connect chromosomes to microtubules. Here we identify conditions that promote Mps1 release from native kinetochore particles isolated from yeast. Our findings suggest how the checkpoint "wait" signals might be turned off when kinetochores bind microtubules.

Author contributions: L.B.K., K.N.O., S.B., and C.L.A. designed research; L.B.K., K.N.O., Y.D., A.B., A.J.L., and N.L. performed research; Y.D., A.B., A.J.L., and N.L. contributed new reagents/analytic tools; L.B.K., K.N.O., Y.D., A.B., A.J.L., N.L., S.B., and C.L.A. analyzed data; and L.B.K., K.N.O., S.B., and C.L.A. wrote the paper.

The authors declare no conflict of interest.

This article is a PNAS Direct Submission.

[1]L.B.K. and K.N.O. contributed equally to this work.

[2]To whom correspondence may be addressed. Email: sbiggins@fredhutch.org or casbury@uw.edu.

This article contains supporting information online at www.pnas.org/lookup/suppl/doi:10.1073/pnas.1901653116/-/DCSupplemental.

Published online August 12, 2019.

release from microtubule-attached kinetochores remain incompletely understood.

To elucidate how the association and dissociation of Mps1 from kinetochores are controlled, we developed a unique reconstitution system using isolated budding yeast kinetochores, which have previously been shown to recapitulate checkpoint signaling events (25, 26) and microtubule tip-coupling activity in vitro (27). Using single-particle microscopy assays, we show that microtubules and Mps1 do not compete directly for association with isolated native kinetochores. Instead, our biochemical assays reveal that Mps1 kinase activity is sufficient for its release from kinetochores. The key substrate appears to be Mps1 itself rather than core kinetochore proteins. Together, these data lead us to propose that biorientation promotes Mps1 autophosphorylation, which decreases the affinity of Mps1 for kinetochores and thus contributes to checkpoint silencing.

Results

Kinetochores Bind Simultaneously to Mps1 and Microtubules In Vitro. We began by testing whether microtubules and Mps1 compete against each other for binding to isolated kinetochores. We previously developed a method to purify kinetochores by immunoprecipitation of the Dsn1 kinetochore protein from budding yeast cells (26, 27). These native kinetochores copurify with a pool of Mps1 that, when activated, is sufficient to recruit the Bub3, Bub1, and Mad1 spindle assembly checkpoint proteins to the kinetochores (25, 26). In addition, association of Mps1 with the native kinetochores requires Ndc80, its kinetochore receptor (*SI Appendix*, Fig. S1*A*) (11). To directly assess the effects of microtubule binding on the kinetochore-bound levels of Mps1, kinetochores purified from cells expressing epitope-tagged Mps1 were incubated with fluorescently labeled Taxol-stabilized microtubules or with unpolymerized tubulin. As negative controls, we also incubated beads lacking kinetochores with microtubules or free tubulin. After incubation, the beads were washed, and the relative levels of fluorescent tubulin and Mps1 that remained bound were analyzed by SDS/PAGE followed by fluorescence imaging and immunoblotting, respectively (Fig. 1*A*). As expected, the kinetochores bound more polymerized tubulin (microtubules) than unpolymerized tubulin, and this binding required the Ndc80 protein (*SI Appendix*, Fig. S1*B*). However, there was no difference in the amount of Mps1 that remained associated with the kinetochores in the presence or absence of microtubule attachments (Fig. 1*A*). These data suggest that kinetochores can simultaneously bind Mps1 and microtubules, in apparent contradiction to a competitive binding model.

A Single-Particle Method to Measure Mps1 Levels on Individual Kinetochores. Because subpopulations of microtubule-bound and -unbound kinetochores could not be distinguished in our initial experiments, we developed a single-particle method to visualize and quantify Mps1 levels on individual kinetochores. We created strains in which endogenous Mps1 and the core kinetochore protein Mtw1 were fused at their C-termini to SNAP and CLIP epitope tags (28, 29), respectively, for labeling with bright, photostable organic fluorophores. Cells expressing Mtw1-CLIP and Mps1-SNAP grew normally and activated the spindle assembly checkpoint in response to the microtubule-destabilizing drug nocodazole, confirming the functionality of the fusion proteins (*SI Appendix*, Fig. S2*A*). Kinetochores isolated from these cells were dyed with SNAP-Surface 549 and CLIP-Surface 647 and then tethered sparsely to coverslips for imaging by multicolor total internal reflection fluorescence (TIRF) microscopy. Most of the particles were single color, carrying Mtw1 but lacking Mps1. Only a small fraction of particles (typically 20 ± 5% or less) were dual color, carrying both Mps1 and Mtw1 (*SI Appendix*, Fig. S2 *C*–*E*). Because Mps1 and Mtw1 molecules at kinetochores are separated by only ~50 nm or less (14), which is below the resolution limit of TIRF

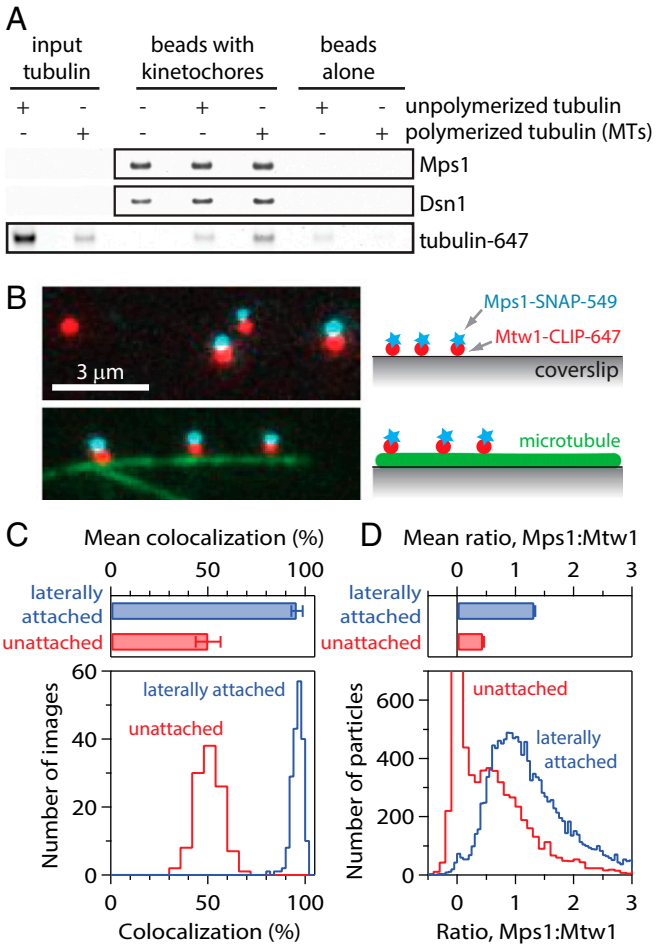

Fig. 1. Isolated kinetochores retain Mps1 when attached laterally to microtubules. (*A*) Kinetochores isolated (from SBY9190) and bound to magnetic beads were mock-treated, incubated with unpolymerized fluorescent tubulin, or incubated with fluorescent Taxol-stabilized microtubules (MTs). The amount of tubulin retained after bead washing was assessed by fluorescence imaging. Kinetochores (represented by Dsn1) and kinetochore-associated Mps1 were detected by immunoblotting. (*B*) Fluorescence images of individual kinetochore particles (from SBY15285) carrying Mps1-SNAP 549 (cyan) and Mtw1-CLIP 647 (red), tethered to a coverslip (*Top*) or attached laterally to a microtubule (green; *Bottom*). Colors are offset vertically; cyan-red pairs are colocalized, dual-color particles. (*C*) Percentages of kinetochore particles retaining Mps1. Bars show mean ± SD values from 192 images of microtubule-attached particles and 112 images of coverslip-tethered particles. Histograms show corresponding distributions. (*D*) Approximate ratios of Mps1 to Mtw1 molecules, estimated from particle brightness relative to the brightness of single Mps1-SNAP 549 and Mtw1-CLIP 647 molecules. Bars show mean ± SEM ratios from 14,189 laterally attached particles and 7,830 coverslip-tethered particles. Histograms show corresponding distributions.

microscopy, their signals overlaid nearly perfectly in raw images. Therefore, to facilitate identification of colocalized particles, the 2 colors are deliberately offset in all the images presented here.

Given the relatively low colocalization, we sought to increase retention of Mps1 with the kinetochores to allow a better dynamic range for our single-particle experiments. We found that kinetochore particles purified from a mutant *dsn1-2D* strain, with phosphomimetic mutations S240D and S250D that have previously been shown to improve recovery of outer kinetochore proteins (30, 31), retained significantly more Mps1. The fraction of phosphomimetic Dsn1-2D particles carrying both Mps1 and Mtw1 was 47 ± 6% (*SI Appendix*, Fig. S2 *C* and *D*), more than double the fraction of wild-type kinetochores carrying both proteins. Particles

with just one detectable Mps1 or Mtw1, identifiable by their single-step photobleaching behavior, served as internal controls, allowing normalization of particle brightness and estimation of the ratio of Mps1 molecules to Mtw1 molecules for each particle. On average, Dsn1-2D kinetochore particles carried a ratio of 0.51 ± 0.02 Mps1 molecules per Mtw1 molecule, and a substantial fraction (20%) were "high-occupancy" (i.e., with 1 or more Mps1 per Mtw1). In contrast, wild-type kinetochore particles carried only 0.11 ± 0.02 Mps1 molecules per Mtw1 molecule on average, and far fewer (3%) were high-occupancy particles (*SI Appendix*, Fig. S2*E*). We confirmed that *dsn1-2D* cells have normal checkpoint function (*SI Appendix*, Fig. S2 *A* and *B*) and used them for subsequent single-particle experiments.

Individual Kinetochores Associate Simultaneously with Mps1 and Microtubules. If Mps1 and microtubules compete directly for binding to kinetochores, then high-occupancy particles, carrying 1 or more Mps1 molecules per Mtw1 molecule, should be inhibited from binding to microtubules. Conversely, the population of particles that bind microtubules should be enriched for low-occupancy particles (i.e., particles with fewer than 1 molecule of Mps1 per Mtw1 molecule). To test this prediction, we anchored Taxol-stabilized microtubules to coverslips, introduced the labeled kinetochores, and then allowed them to bind the sides of the filaments (Fig. 1*B*) (27, 29). Contrary to our expectation, microtubule-bound kinetochores had an even higher average Mps1 occupancy than unbound particles. The fraction of microtubule-bound kinetochores that carried Mps1 was 96 ± 3% (Fig. 1*C*), roughly double that of the control unbound population (50 ± 3%). The microtubule lattice-bound kinetochores also carried a higher ratio of Mps1 molecules per Mtw1 molecule, 1.33 ± 0.01 on average, which was 3-fold higher than the ratio of 0.45 ± 0.01 measured for the control unbound population (Fig. 1*D*). Thus, microtubule attachment appears to select for, rather than against, the high-occupancy particles. We speculate that this higher retention of Mps1 might occur because binding to microtubules selects for more complete kinetochore particles.

To confirm that the simultaneous association of Mps1 and microtubules with kinetochores was not related to the Dsn1-2D mutant, we also analyzed wild-type kinetochores. Although the particles from a wild-type Dsn1 strain retained less Mps1 than seen in Dsn1-2D particles, they nevertheless bound microtubules independently of whether or not they carried Mps1 (*SI Appendix*, Fig. S3). These observations indicate that isolated yeast kinetochores can associate simultaneously with Mps1 and with the microtubule lattice in a noncompetitive manner.

While kinetochores initially associate with the lateral sides of microtubules, they convert to end-on attachments upon biorientation. Because the checkpoint is apparently silenced only after bioriented, end-on attachments are made (32), we developed a single-particle technique to analyze Mps1 association specifically with tip-attached kinetochores. Purified, labeled kinetochores were tethered to coverslips, and fluorescent Taxol-stabilized microtubules were introduced into the chamber. Through thermal diffusion, the microtubules tended to attach via their ends to the kinetochores (Fig. 2*A*). Surface-tethered kinetochores in the same fields of view that failed to capture a microtubule served as internal controls. Nearly all of the kinetochores that captured microtubule ends (93 ± 21%) retained Mps1 (Fig. 2*B*). A smaller fraction of the control, unattached particles (35 ± 14%) retained Mps1, similar to our previous results without microtubules (Fig. 1). These data suggest that Mps1 does not compete specifically with microtubule tips.

Individual Kinetochores Tracking Disassembling Microtubule Tips Retain Mps1. Bioriented kinetochores in vivo attach persistently to dynamic microtubule tips, an arrangement that allows them to harness tip disassembly to drive chromosome movement (33, 34)

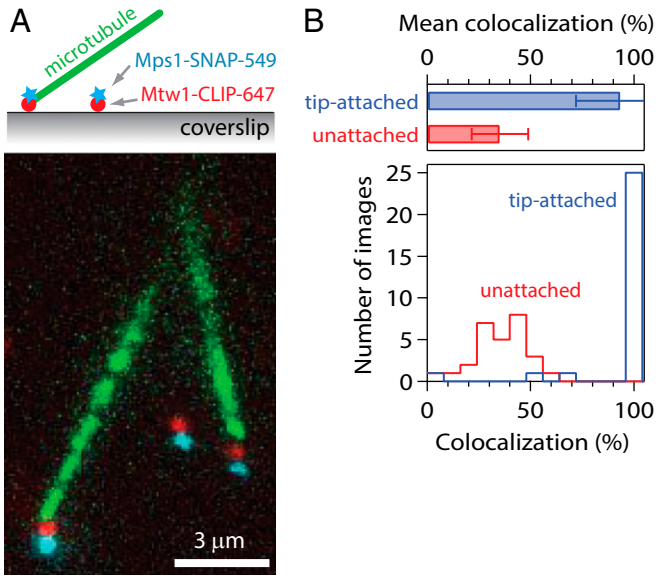

Fig. 2. Kinetochores retain Mps1 when attached to microtubule tips. (*A*) Fluorescence image of kinetochore particles (from SBY15285) carrying Mps1-SNAP 549 (cyan) and Mtw1-CLIP 647 (red) tethered to a coverslip and exposed to free, Taxol-stabilized Alexa Fluor 488 microtubules (green). By thermal diffusion, the filaments attached via their tips to the coverslip-tethered kinetochores. Colors are offset vertically; cyan-red pairs are colocalized, dual-color kinetochore particles. (*B*) Percentages of kinetochore particles retaining Mps1. Bars show mean ± SD values from 28 images of 40 tip-attached particles and 366 coverslip-tethered particles. Histograms show the corresponding distributions of colocalization measured for the tip-attached and coverslip-tethered particles in each individual image.

and that also might be important for silencing their checkpoint signals. To examine whether dynamic tip attachments are required to exclude Mps1 from kinetochores, we grew microtubules from coverslip-anchored seeds and allowed purified, labeled kinetochores to attach laterally to the growing filaments. We then triggered microtubule disassembly by rapid buffer exchange to remove the free tubulin (Fig. 3*A*). When disassembling tips encountered individual kinetochore particles, the particles began tracking with the tips and were usually carried all the way to the coverslip-anchored seed (Fig. 3*B* and Movie S1), as reported previously (27). Nearly all the tip-tracking particles (95 ± 22%) retained Mps1 throughout their movement (Fig. 3*C*). A similarly high level of Mps1 retention (93 ± 11%) was seen for laterally attached particles in the same fields of view (Fig. 3*C*), consistent with the experiments using Taxol-stabilized filaments. These data show that Mps1 does not compete with dynamic microtubule tips for binding to isolated kinetochores.

Activating Mps1 Triggers Its Release from Kinetochores. Microtubule binding did not release Mps1 from kinetochores in our reconstitution experiments, yet Mps1 levels are clearly reduced on bioriented vs. unattached kinetochores in cells (7, 12, 14). Previous research in human cells found that attenuating Mps1 activity with inhibitors increased the level of kinetochore-associated Mps1 and also reduced Mps1 turnover at kinetochores, suggesting that Mps1 release from kinetochores is phosphoregulated (13, 20–23, 35, 36). In addition, mutational analyses found that Mps1 autophosphorylation regulates its localization to kinetochores, but there were conflicting observations on whether this autophosphorylation aids or inhibits its kinetochore association (17, 23, 37). We hypothesized that Mps1 activity might be sufficient to promote its release from isolated kinetochores in vitro, and we were able to test this because Mps1 is the primary kinase activity that copurifies with the

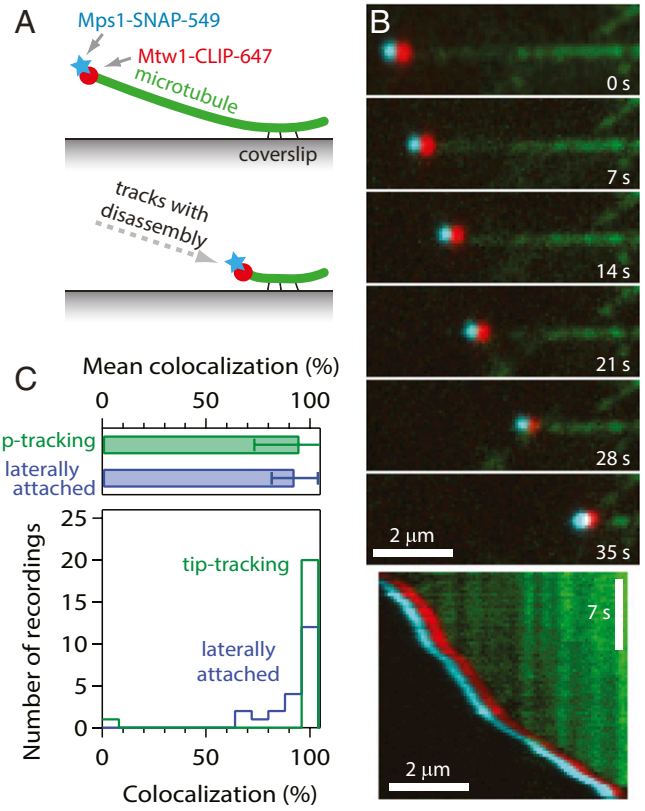

Fig. 3. Kinetochores retain Mps1 when tracking with disassembling microtubule tips. (*A*) Schematic of the experiment. Dynamic microtubule extensions were grown from coverslip-anchored seeds and decorated with kinetochore particles. Disassembly was then induced by buffer exchange to remove free tubulin. (*B*) Selected frames (*Top*) and kymograph (*Bottom*) from Movie S1 showing a kinetochore particle (from SBY15285) tracking with the disassembling tip of a microtubule (green) and carrying Mps1-SNAP 549 (cyan) and Mtw1-CLIP 647 (red). Colors are offset horizontally; the cyan-red pair is a colocalized, dual-color kinetochore particle. (*C*) Percentages of kinetochore particles retaining Mps1. Bars show mean ± SD values from 21 recordings of 32 tip-tracking particles and 213 laterally attached particles. Histograms show corresponding distributions.

isolated yeast kinetochores (26). To do this, we purified kinetochores carrying Mps1-SNAP and Mtw1-CLIP, dyed them, and then treated them with or without ATP. We analyzed Mps1 levels that remained associated with the ATP-treated kinetochores, as well as the levels that were released into the supernatants via fluorescent gel imaging. ATP treatment was sufficient to release Mps1 from the purified kinetochores, and the electrophoretic mobility of the released Mps1 was clearly reduced (Fig. 4*A*), suggesting that it had become phosphorylated. To confirm that the mobility shift was due to phosphorylation, we purified Mps1 itself, treated it with ATP, and then added λ-phosphatase. Indeed, an ATP-dependent mobility shift occurred and was eliminated by phosphatase treatment (Fig. 4*B*). These results show that activating kinetochore-associated Mps1 triggers its autophosphorylation, as well as its release from kinetochores.

Autophosphorylation Reduces the Affinity of Mps1 for Kinetochores. Mps1 phosphorylates itself and also several major kinetochore proteins in vitro (11, 26), including Ndc80, making it unclear whether the dissociation of Mps1 was due to phosphorylation of sites on Mps1 itself, on other kinetochore proteins, or on both. To distinguish among these possibilities, we independently manipulated the phosphorylation states of isolated kinetochores and Mps1 and then tested whether they would associate in vitro.

We first tested whether Mps1-mediated phosphorylation of kinetochores alters their affinity for Mps1. We created phosphorylated kinetochores lacking endogenous Mps1 by incubating purified kinetochores with ATP (Fig. 4*C*). Immunoblotting confirmed the release of endogenous Mps1 (*SI Appendix*, Fig. S4*A*), and an electrophoretic mobility shift of Spc105, a known Mps1 substrate (26), served as a readout for kinetochore phosphorylation by Mps1 (Fig. 4*D*). To create dephosphorylated kinetochores for use as controls, we divided the ATP-treated kinetochores and treated one-half with λ-phosphatase (Fig. 4*C*). The phosphorylated and dephosphorylated kinetochores were then incubated with exogenous Mps1 (~97 kD) that had been purified separately under high stringency conditions from asynchronously growing yeast cells (*SI Appendix*, Fig. S4*B*). We found that similar amounts of exogenous Mps1 bound to the kinetochores regardless of their phosphorylation state (Fig. 4*D*), indicating that kinetochore phosphorylation by Mps1 does not inhibit Mps1 from associating with kinetochores.

To test whether the affinity of Mps1 for kinetochores is reduced specifically by autophosphorylation, we generated autophosphorylated Mps1 and tested its binding to dephosphorylated kinetochores lacking endogenous Mps1 (Fig. 4*C*). To obtain autophosphorylated Mps1 (P-Mps1), we purified the native kinase and incubated it with ATP (*SI Appendix*, Fig. S4*B*). We prepared dephosphorylated kinetochores lacking endogenous Mps1 as described above by sequentially treating them with ATP to release Mps1 and then λ-phosphatase to remove phosphorylation (*SI Appendix*, Fig. S5). We incubated the kinetochores with the Mps1 that was either untreated or autophosphorylated. Strikingly, while native untreated Mps1 bound well to the kinetochores, the autophosphorylated P-Mps1 bound poorly (Fig. 4*E* and *SI Appendix*, Fig. S5). Only a minor subfraction bound to the kinetochores, and its electrophoretic mobility was faster than that of the major unbound fraction, indicating that the kinetochores selectively bound less-phosphorylated forms of Mps1. These results demonstrate that autophosphorylated forms of Mps1 have lower affinity for kinetochores and suggest that autophosphorylation underlies the release of Mps1 from yeast kinetochores.

Discussion

Mps1 initiates and sustains the spindle assembly checkpoint, so understanding the regulation of its activity is paramount to understanding checkpoint function. Together, the release of Mps1 from bioriented kinetochores in vivo (12, 14, 16) and the evidence that the duration of checkpoint signaling is correlated with Mps1 kinetochore localization (13–15) strongly suggest that controlling the binding and release of Mps1 to and from kinetochores is key to regulating the spindle assembly checkpoint. Here, by developing in vitro assays to monitor spindle assembly checkpoint protein colocalization with isolated yeast kinetochore particles, we show that native, kinetochore-bound Mps1 does not interfere with attachment of the kinetochores to microtubules in several different configurations, arguing against the direct competition mechanism for checkpoint silencing.

Given the dynamic association of Mps1 with kinetochores in cells, the stability of its association with isolated kinetochores in vitro is striking. Our kinetochore isolation procedure requires >60 min for the resuspension of cell lysate, anti-FLAG immunoprecipitation, washing away of free proteins, and then FLAG-peptide elution. Therefore, retention of Mps1 on 20% to 50% of the eluted particles implies a very low spontaneous release rate, roughly 1 to 3 h^{-1}. In contrast, fluorescence recovery after photobleaching (FRAP) measurements indicate that turnover in vivo occurs much faster, at rates of 5 to 20 min^{-1} (12, 13). The slower turnover after isolation of the kinetochores is presumably caused, at least in part, by a lack of ATP, since treating the kinetochores with ATP triggers Mps1 release. This implies that fast turnover in vivo is likely an active, ATP-dependent process.

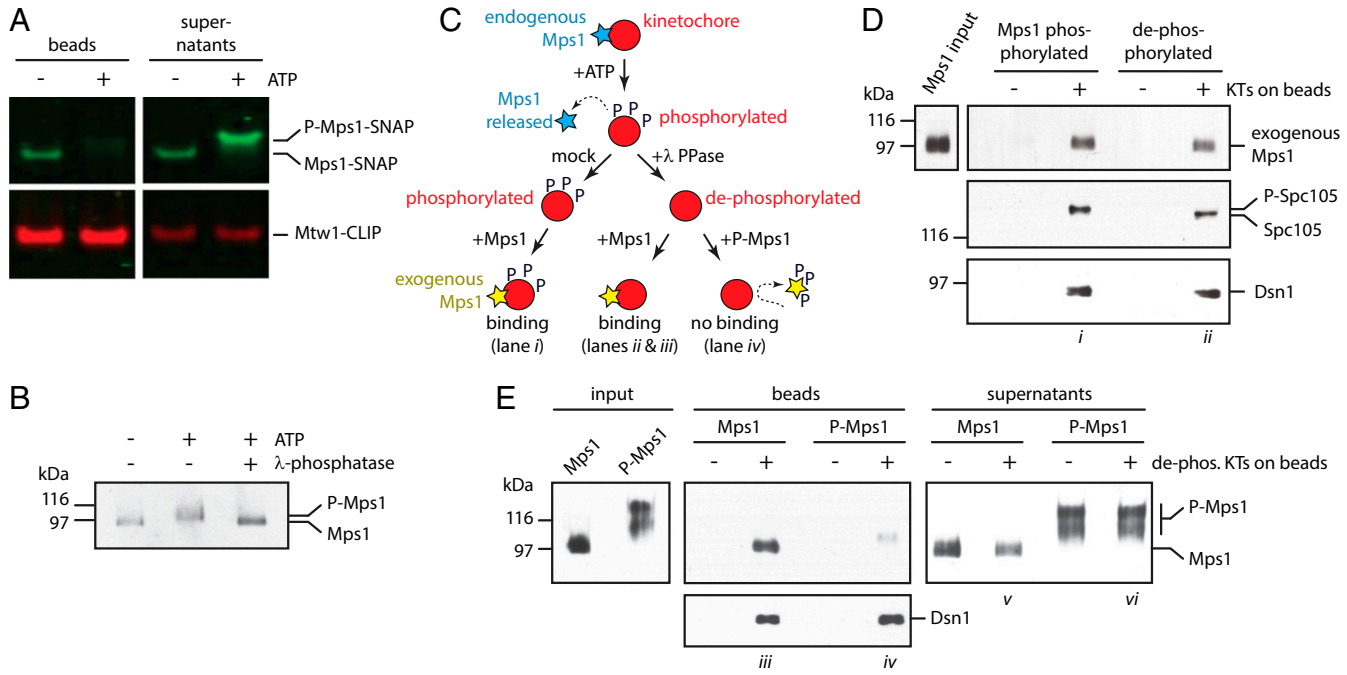

Fig. 4. Mps1 autophosphorylation inhibits its binding to kinetochores. (*A*) An in vitro kinase reaction releases Mps1 from isolated kinetochores. Kinetochores carrying Mps1-SNAP 549 (green) and Mtw1-CLIP 647 (red) (from SBY15285) were immunoprecipitated on magnetic beads and incubated with or without ATP. Proteins retained on beads and released into the supernatants were analyzed by SDS/PAGE and fluorescence imaging. (*B*) The electrophoretic mobility shift caused by incubation of Mps1 with ATP is due to phosphorylation. Mps1 was purified (from SBY12412) via immunoprecipitation under stringent conditions to remove copurifying proteins and then incubated with or without ATP. An aliquot of the ATP-treated sample was subsequently treated with λ-phosphatase. The resulting samples were analyzed by immunoblotting. (*C*) Schematic illustrating the preparation of Mps1-phosphorylated and dephosphorylated kinetochores for binding to exogenous Mps1. (*D*) Mps1 binds equivalently to Mps1-phosphorylated or dephosphorylated kinetochores. Kinetochores (from SBY9190) and control beads lacking kinetochores were prepared, incubated with purified exogenous Mps1 (from SBY12412, as diagrammed in *C*), washed, and then analyzed by immunoblotting. (*E*) Autophosphorylated Mps1 fails to bind kinetochores. Immobilized kinetochores (from SBY9190) and beads lacking kinetochores were treated sequentially with ATP and then λ-phosphatase to release endogenous Mps1 and remove phosphates. They were then washed and incubated with native Mps1 or with autophosphorylated P-Mps1 (from SBY12412, as diagrammed in *C*). Native Mps1 that had not been autophosphorylated in vitro bound well to the kinetochores (lane *iii*), with some excess remaining in the supernatant (lane *v*). Autophosphorylated P-Mps1 bound poorly (lane *iv*). Electrophoretic mobility of the minor, kinetochore-bound P-Mps1 subfraction (lane *iv*) was faster than that of the major unbound fraction (lane *vi*), indicating that kinetochores selectively bind less-phosphorylated forms of Mps1.

Indeed, prior work in human cells has shown that chemical inhibition of Mps1 causes its accumulation at kinetochores (13, 20–23, 35), and that phosphomimetic mutations in Mps1 reduce its levels at kinetochores (23). Taken together, these observations suggest that Mps1 autophosphorylation promotes its release from kinetochores. Our findings provide direct support for this view and reveal that Mps1 autorelease only requires components stably associated with kinetochores (and ATP). Autophosphorylation of Mps1 kinase could be a conserved mechanism for promoting its release from kinetochores. However, some evidence suggests that autophosphorylation of human Mps1 might promote its interaction with, rather than its release from, the core kinetochore component Ndc80 (17, 37). Given that Mps1 is heavily phosphorylated in mitotic cells, it seems possible that autophosphorylation of some sites might promote kinetochore localization while phosphorylation of others might promote release (7, 8, 13, 17, 18, 37–39). In the future, it will be crucial to identify the key autoregulatory phosphorylation sites to determine specifically how they affect Mps1 association with and release from kinetochores.

Two previous elegant studies have demonstrated that recombinant fragments of human Mps1 compete directly against Taxol-stabilized microtubules for binding to human Ndc80/Hec1 complex (17, 18). There are at least 2 possible explanations for the absence of such direct competition at the level of whole yeast kinetochore particles. First, checkpoint silencing might rely on direct competition in humans but not in yeast. While such an interspecies difference is formally possible, we do not favor this explanation, because the Ndc80 complex is a widely conserved microtubule-binding element that recruits Mps1 in both organisms. Another possibility is that Mps1 might interact with kinetochores in more than one way, and the native purified kinetochores might selectively retain only a noncompetitive fraction. Consistent with this possibility, multiple types of kinetochore interactions have been observed for human Mps1 (18, 35, 40, 41). While further work is needed to determine whether this is the case for yeast Mps1, our previous reconstitutions of key Mps1-dependent checkpoint-triggering phosphorylation events strongly suggest that the pool of Mps1 carried by the isolated yeast kinetochore particles is physiologically relevant (25, 26).

Our results lead us to speculate that molecular or physical events occurring when sister kinetochores make end-on bioriented attachments might stimulate Mps1 autophosphorylation and thus release. In support of this possibility, a previous study found that microtubules stimulate Mps1 kinase activity in vitro (42). Perhaps when a kinetochore binds a microtubule, interactions between the kinetochore-associated Mps1 and the microtubule might enable Mps1 autophosphorylation, lowering its affinity for Ndc80 and thereby causing its release from the kinetochore. Alternatively, conformational changes in the kinetochore (14) that occur when it attaches to a microtubule might directly promote Mps1 autophosphorylation. Recent work has suggested that Mps1 is prevented from reaching its checkpoint substrate KNL1/Spc105 when kinetochores bind to microtubules (14). Thus, conformational changes in the kinetochore caused by microtubule binding or tension could

silence Mps1 checkpoint activity in 2 distinct ways; they might simultaneously block Mps1 activity toward checkpoint substrates and redirect its activity toward itself, triggering its own release from the kinetochore. Consistent with the idea of heightened Mps1 autoactivity during checkpoint silencing, FRAP data suggest that Mps1 is more dynamic on metaphase kinetochores compared with prometaphase kinetochores in mammalian cells (12). A model in which overall checkpoint activity is tuned by the phosphorylation state of Mps1 fits well with the kinetic evidence demonstrating that spindle assembly checkpoint signaling is graded rather than switch-like (reviewed in ref. 2). A graded regulation of Mps1 kinetochore localization, which favors a decrease in Mps1 affinity rather than its complete loss from kinetochores, might also facilitate rapid checkpoint reactivation should an attachment be lost. In the future, the in vitro assays that we have established here should be useful for further understanding how microtubule attachment affects the activity and kinetochore localization of Mps1 and other checkpoint proteins.

Methods

Native kinetochores were purified by immunoprecipitation from asynchronously growing yeast as described previously (27) with modifications to the lysis as described previously (43), and then labeled with fluorescent dyes (29). Native Mps1 was purified in essentially the same manner. For examining the levels of Mps1 on individual, unattached kinetochore particles, the fluorescent kinetochores were tethered sparsely to coverslips. For examining Mps1 levels on laterally attached kinetochore particles, the kinetochores were incubated with Taxol-stabilized microtubules that had been anchored to coverslips. To examine tip-attached kinetochores, kinetochore particles tethered sparsely to coverslips were incubated with short, Taxol-stabilized microtubules, which tended to attach to the coverslip-tethered kinetochores by their ends. To examine tip-tracking particles, dynamic microtubule extensions were grown from coverslip-anchored seeds in the presence of free kinetochores and then tubulin was removed by buffer exchange, to trigger microtubule disassembly. Kinetochores that had attached laterally to the microtubule extensions were captured and carried by the disassembling tips. For all single-particle experiments, images were recorded using an automated multicolor TIRF microscope (44) and analyzed using custom routines written in LabView (National Instruments) and Igor Pro (WaveMetrics). Additional details of the purification, fluorescent labeling, and imaging of the native kinetochores, along with descriptions of the kinase and bulk binding assays, are provided in *SI Appendix, Methods*.

ACKNOWLEDGMENTS. We thank Geert Kops and Hongtao Yu for communicating results and useful discussions; Arshad Desai, Aaron Hoskins, Leon Chan, and Mark Winey for providing reagents; and Justin Kollman, John Tuthill, members of the Seattle Mitosis Group, and the C.L.A. and S.B. labs for helpful discussions and comments on the manuscript. L.B.K. was supported by an NSF graduate research fellowship (DGE-1256082). K.N.O. was supported by an NIH training fellowship (T32GM007270). N.L. was supported by an NIH interdisciplinary training grant (T32CA080416). This work was supported by Packard Fellowship 2006-30521 (to C.L.A.); by NIH Grants R01 GM079373 (to C.L.A.), P01 GM105537 (to C.L.A.), and R01 GM064386 (to S.B.); and by the Genomics and Scientific Imaging Shared Resources of the Fred Hutchinson/University of Washington Cancer Consortium (P30 CA015704). S.B. is an investigator of the Howard Hughes Medical Institute.

1. D. J. Gordon, B. Resio, D. Pellman, Causes and consequences of aneuploidy in cancer. *Nat. Rev. Genet.* **13**, 189–203 (2012).
2. N. London, S. Biggins, Signalling dynamics in the spindle checkpoint response. *Nat. Rev. Mol. Cell Biol.* **15**, 736–747 (2014).
3. A. Musacchio, The molecular biology of spindle assembly checkpoint signaling dynamics. *Curr. Biol.* **25**, R1002–R1018 (2015).
4. C. L. Rieder, H. Maiato, Stuck in division or passing through: What happens when cells cannot satisfy the spindle assembly checkpoint. *Dev. Cell* **7**, 637–651 (2004).
5. G. J. Kops, B. A. Weaver, D. W. Cleveland, On the road to cancer: Aneuploidy and the mitotic checkpoint. *Nat. Rev. Cancer* **5**, 773–785 (2005).
6. X. Liu, M. Winey, The MPS1 family of protein kinases. *Annu. Rev. Biochem.* **81**, 561–585 (2012).
7. S. T. Liu *et al*., Human MPS1 kinase is required for mitotic arrest induced by the loss of CENP-E from kinetochores. *Mol. Biol. Cell* **14**, 1638–1651 (2003).
8. W. J. Palframan, J. B. Meehl, S. L. Jaspersen, M. Winey, A. W. Murray, Anaphase inactivation of the spindle checkpoint. *Science* **313**, 680–684 (2006).
9. K. G. Hardwick, E. Weiss, F. C. Luca, M. Winey, A. W. Murray, Activation of the budding yeast spindle assembly checkpoint without mitotic spindle disruption. *Science* **273**, 953–956 (1996).
10. S. Martin-Lluesma, V. M. Stucke, E. A. Nigg, Role of Hec1 in spindle checkpoint signaling and kinetochore recruitment of Mad1/Mad2. *Science* **297**, 2267–2270 (2002).
11. S. Kemmler *et al*., Mimicking Ndc80 phosphorylation triggers spindle assembly checkpoint signalling. *EMBO J.* **28**, 1099–1110 (2009).
12. B. J. Howell *et al*., Spindle checkpoint protein dynamics at kinetochores in living cells. *Curr. Biol.* **14**, 953–964 (2004).
13. N. Jelluma, T. B. Dansen, T. Sliedrecht, N. P. Kwiatkowski, G. J. Kops, Release of Mps1 from kinetochores is crucial for timely anaphase onset. *J. Cell Biol.* **191**, 281–290 (2010).
14. P. Aravamudhan, A. A. Goldfarb, A. P. Joglekar, The kinetochore encodes a mechanical switch to disrupt spindle assembly checkpoint signalling. *Nat. Cell Biol.* **17**, 868–879 (2015).
15. J. Maciejowski *et al*., Mps1 regulates kinetochore-microtubule attachment stability via the Ska complex to ensure error-free chromosome segregation. *Dev. Cell* **41**, 143–156.e6 (2017).
16. Z. Dou *et al*., Dynamic distribution of TTK in HeLa cells: Insights from an ultrastructural study. *Cell Res.* **13**, 443–449 (2003).
17. Y. Hiruma *et al*., Competition between MPS1 and microtubules at kinetochores regulates spindle checkpoint signaling. *Science* **348**, 1264–1267 (2015).
18. Z. Ji, H. Gao, H. Yu, Kinetochore attachment sensed by competitive Mps1 and microtubule binding to Ndc80C. *Science* **348**, 1260–1264 (2015).
19. M. Moura *et al*., Protein phosphatase 1 inactivates Mps1 to ensure efficient spindle assembly checkpoint silencing. *eLife* **6**, e25366 (2017).
20. L. Hewitt *et al*., Sustained Mps1 activity is required in mitosis to recruit O-Mad2 to the Mad1-C-Mad2 core complex. *J. Cell Biol.* **190**, 25–34 (2010).
21. N. Kwiatkowski *et al*., Small-molecule kinase inhibitors provide insight into Mps1 cell cycle function. *Nat. Chem. Biol.* **6**, 359–368 (2010).
22. T. Sliedrecht, C. Zhang, K. M. Shokat, G. J. Kops, Chemical genetic inhibition of Mps1 in stable human cell lines reveals novel aspects of Mps1 function in mitosis. *PLoS One* **5**, e10251 (2010).
23. X. Wang *et al*., Dynamic autophosphorylation of Mps1 kinase is required for faithful mitotic progression. *PLoS One* **9**, e104723 (2014).
24. R. Colombo *et al*., Targeting the mitotic checkpoint for cancer therapy with NMS-P715, an inhibitor of MPS1 kinase. *Cancer Res.* **70**, 10255–10264 (2010).
25. N. London, S. Biggins, Mad1 kinetochore recruitment by Mps1-mediated phosphorylation of Bub1 signals the spindle checkpoint. *Genes Dev.* **28**, 140–152 (2014).
26. N. London, S. Ceto, J. A. Ranish, S. Biggins, Phosphoregulation of Spc105 by Mps1 and PP1 regulates Bub1 localization to kinetochores. *Curr. Biol.* **22**, 900–906 (2012).
27. B. Akiyoshi *et al*., Tension directly stabilizes reconstituted kinetochore-microtubule attachments. *Nature* **468**, 576–579 (2010).
28. A. A. Hoskins *et al*., Ordered and dynamic assembly of single spliceosomes. *Science* **331**, 1289–1295 (2011).
29. K. K. Sarangapani *et al*., Sister kinetochores are mechanically fused during meiosis I in yeast. *Science* **346**, 248–251 (2014).
30. B. Akiyoshi, C. R. Nelson, S. Biggins, The Aurora B kinase promotes inner and outer kinetochore interactions in budding yeast. *Genetics* **194**, 785–789 (2013).
31. Y. N. Dimitrova, S. Jenni, R. Valverde, Y. Khin, S. C. Harrison, Structure of the MIND complex defines a regulatory focus for yeast kinetochore assembly. *Cell* **167**, 1014–1027.e12 (2016).
32. J. Kuhn, S. Dumont, Spindle assembly checkpoint satisfaction occurs via end-on but not lateral attachments under tension. *J. Cell Biol.* **216**, 1533–1542 (2017).
33. S. Inoué, E. D. Salmon, Force generation by microtubule assembly/disassembly in mitosis and related movements. *Mol. Biol. Cell* **6**, 1619–1640 (1995).
34. D. E. Koshland, T. J. Mitchison, M. W. Kirschner, Polewards chromosome movement driven by microtubule depolymerization in vitro. *Nature* **331**, 499–504 (1988).
35. Z. Dou *et al*., Dynamic localization of Mps1 kinase to kinetochores is essential for accurate spindle microtubule attachment. *Proc. Natl. Acad. Sci. U.S.A.* **112**, E4546–E4555 (2015).
36. S. Santaguida, A. Tighe, A. M. D'Alise, S. S. Taylor, A. Musacchio, Dissecting the role of MPS1 in chromosome biorientation and the spindle checkpoint through the small molecule inhibitor reversine. *J. Cell Biol.* **190**, 73–87 (2010).
37. Q. Xu *et al*., Regulation of kinetochore recruitment of two essential mitotic spindle checkpoint proteins by Mps1 phosphorylation. *Mol. Biol. Cell* **20**, 10–20 (2009).
38. W. Nijenhuis *et al*., A TPR domain-containing N-terminal module of MPS1 is required for its kinetochore localization by Aurora B. *J. Cell Biol.* **201**, 217–231 (2013).
39. V. Morin *et al*., CDK-dependent potentiation of MPS1 kinase activity is essential to the mitotic checkpoint. *Curr. Biol.* **22**, 289–295 (2012).
40. S. T. Pachis, G. J. P. L. Kops, Leader of the SAC: Molecular mechanisms of Mps1/TTK regulation in mitosis. *Open Biol.* **8**, 180109 (2018).
41. S. T. Pachis, Y. Hiruma, E. C. Tromer, A. Perrakis, G. Kops, Interactions between N-terminal modules in MPS1 enable spindle checkpoint silencing. *Cell Rep.* **26**, 2101–2112.e6 (2019).
42. V. M. Stucke, C. Baumann, E. A. Nigg, Kinetochore localization and microtubule interaction of the human spindle checkpoint kinase Mps1. *Chromosoma* **113**, 1–15 (2004).
43. M. P. Miller, C. L. Asbury, S. Biggins, A TOG protein confers tension sensitivity to kinetochore-microtubule attachments. *Cell* **165**, 1428–1439 (2016).
44. Y. Deng, C. L. Asbury, Simultaneous manipulation and super-resolution fluorescence imaging of individual kinetochores coupled to microtubule tips. *Methods Mol. Biol.* **1486**, 437–467 (2017).

PNAS
www.pnas.org

Supplementary Information for

Autophosphorylation is sufficient to release Mps1 kinase from native kinetochores

Lori B. Koch, Kwaku N. Opoku, Yi Deng, Adrienne Barber, Aimee J. Littleton, Nitobe London, Sue Biggins, Charles L. Asbury.

Correspondence: casbury@uw.edu; sbiggins@fredhutch.org

This PDF file includes:

Supplementary Methods
Supplementary Figures S1 to S5
Supplementary Tables S1 to S3
Caption for Supplementary Movie S1
Supplementary References

Other supplementary materials for this manuscript include the following:

Supplementary Movie S1

www.pnas.org/cgi/doi/10.1073/pnas.1901653116

Supplementary Methods

Yeast strain and plasmid construction

Saccharomyces cerevisiae strains used in this study are isogenic with the W303 background and described in Supplementary Table S1. Standard genetic techniques were used. *DSN1-6His-3Flag* is described in (1). *MPS1-3V5, PDS1-18Myc,* and *DSN1-3Flag* were made by a PCR-based integration system and confirmed by PCR (6, 7). A strain with *NDC80-3V5-IAA17:KANMX* was made using a standard PCR-based integration system with primers SB1510 and SB1511 and template pSB2067, a gift from Leon Chan, Weis Lab. This strain was subsequently crossed several times and SBY12352 is a derivative. The auxin degron tagging system is described in (8). Strains with *mps1Δ::KanMX:10Myc-MPS1:TRP1* were made by crossing a strain, 2964, provided by Mark Winey (SBY3857). Strains with *MPS1-SNAP* were made by crossing an MTW1-CLIP, DSN1-6His-3FLAG strain from our previous work (SBY10327) with a strain, SBY12459, made using a standard PCR-based integration system with primers SB4170 and SB4171 and template pSB1821 (3, 9). *Dsn1-2D-6His-3Flag* strains were made by crossing to a strain made by transformation of a PCR product from plasmid pSB2439 with primers SB654 and SB2435. All strains and corresponding protocols are available by request.

Spindle assembly checkpoint silencing assays

Spindle assembly checkpoint silencing assays were performed by arresting cells with 10 µg/ml nocodazole for 2 hours, washing cells 3 times in fresh media lacking nocodazole, then resuspending cells in YPDA (YEP + 2% glucose + 0.02% adenine) and taking samples at the indicated times. 1 µg/ml alpha factor was added to the cultures 40-50 minutes after the beginning of the time course to prevent cells from entering a second cell cycle. All experiments were repeated at least 2-3 times.

Purification of native kinetochore particles and Mps1

Kinetochore particles were purified from asynchronously growing yeast by anti-Flag IP of Dsn1-6His-3Flag or Dsn1-3Flag as described in (1) with modifications to the lysis method described in (2). Mps1 was purified from asynchronously growing yeast by anti-V5 IP of Mps1-3V5. Cells

were grown to mid-log in yeast extract peptone dextrose media (YPD) supplemented with 0.2 mM adenine. After harvesting cells, they were washed once in water with 2 mM PMSF and then once in buffer H (25 mM HEPES pH 8.0, 2 mM $MgCl_2$, 0.1 mM EDTA, 0.5 mM EGTA, 0.1% NP-40, 15% glycerol with 150 mM KCl for kinetochores or 750 mM KCl for Mps1) with protease inhibitors (at 20 µg/mL final concentration for each of leupeptin, pepstatin A, chymostatin and 200 µM phenylmethylsulfonyl fluoride) and phosphatase inhibitors (0.1 mM Na-orthovanadate, 0.2 µM microcystin, 2 mM β-glycerophosphate, 1 mM Na pyrophosphate, 5 mM NaF). Pelleted cells were resuspended in buffer H (with 150 mM KCl for kinetochores and 750 mM KCl for Mps1) with protease inhibitors and phosphatase inhibitors and then added dropwise to liquid nitrogen to flash freeze. Flash frozen resuspended lysate was processed in a Freezer/Mill (SPEX SamplePrep) submerged in liquid nitrogen and the lysate was clarified by ultracentrifugation at 98,500 g for 90 min at 4 °C. Anti-Flag or anti-V5 conjugated Protein G Dynabeads (Thermo Fisher #100.09D) were incubated with the appropriate lysates for 3 hours with constant rotation at 4 °C, followed by 3 washes with buffer H containing protease inhibitors, phosphatase inhibitors, 2 mM dithiothreitol (DTT) and either 0.15 M KCl (kinetochores) or 1 M KCl (Mps1). Next, beads were washed twice with buffer H containing 150 mM KCl and protease inhibitors. Proteins were eluted from the beads by gentle agitation in elution buffer (0.5 mg/ml 3Flag peptide or 0.5 mg/ml 3V5 peptide in buffer H with 0.15 M KCl and protease inhibitors) for 25 min at room temperature or by boiling in SDS sample buffer. The concentrations of purified kinetochores and Mps1 were determined by comparing the purified material with BSA standards on silver-stained SDS-PAGE gels.

Bulk kinetochore-microtubule binding assay

Alexa 647-labeled microtubules were polymerized by incubating a 1:50 mixture of Alexa 647-labeled bovine tubulin to unlabeled bovine tubulin in polymerization buffer (80 mM PIPES, 1.2 mM $MgCl_2$, 1 mM GTP, 5.7% (v/v) DMSO, 1 mM EGTA pH 6.8). Following polymerization, taxol was added to a final concentration of 10 µM and the microtubules were sheared by passing the solution through a 27½ G needle 10 times. Microtubules were pelleted by centrifugation at 170,000 g for 10 minutes at 23 °C and resuspended in BRB80 with 20 µM taxol. Following the standard purification protocol, kinetochores maintained on beads or mock-treated beads were washed once with 1X BRB80 (80 mM PIPES, 1 mM $MgCl_2$, 1 mM EGTA, pH 6.8) with 20 µM

taxol. To perform the binding assay, the beads were then incubated in 1X BRB80 supplemented with 1 mg/ml κ-casein, 20 μM taxol and either unpolymerized tubulin (0.05 mg/ml final concentration) or taxol-stabilized microtubules (0.009 mg/ml final concentration) with constant rotation for 25 minutes at room temperature. The concentration of microtubules added to the reactions was calculated by comparing the fluorescent intensity of unpolymerized tubulin and the taxol-stabilized microtubule tubulin on an SDS-PAGE gel imaged with a Typhoon Trio (GE Healthcare). Following the binding reaction, the beads were washed once in BRB80 with 20 μM taxol and then the bead-associated proteins eluted by boiling in SDS sample buffer. The kinetochore proteins Dsn1 and Mps1 were visualized by immunoblotting.

Immunoblot Analysis

Immunoblotting and detection using chemiluminescence was performed as described in (2). Commercial antibodies used for immunoblotting were: 9E10 (Covance) at a 1:10,000 dilution for the Myc tag, anti-Flag M2 antibodies (Sigma-Aldrich) at 1:3,000, anti-Pgk1 antibodies (Invitrogen) at 1:10,000, anti-V5 (Invitrogen) at 1:5,000, and rat anti-alpha-tubulin (Accurate Chemical & Scientific) at 1:1,000. Anti-Spc105 antibodies were used at 1:10,000 (1). The anti-Ndc80 antibodies (OD4) were a kind gift from Arshad Desai and were used at a 1:10,000 dilution.

Isolation of fluorescent kinetochore particles

For direct observation of Mps1 levels by fluorescence, we isolated kinetochore particles from yeast strains in which Mps1 and a core kinetochore protein, Mtw1, were tagged with SNAP and CLIP, respectively. These tags allowed the proteins to be efficiently labeled with bright, photostable fluorescent dyes, CLIP-Surface 647 and SNAP-Surface 549 (New England Biolabs), during kinetochore purification. Kinetochores were purified as described above, with the following modifications for fluorescent labeling. After immunoprecipitation of the kinetochores onto magnetic beads, the beads were washed three times in buffer H supplemented with 2 mM dithiothreitol (DTT) and then two times in buffer H/0.15 lacking DTT. The kinetochores were then labeled by suspension in buffer H/0.15 plus 30 μM SNAP-Surface-549 and 30 μM CLIP-Surface-647 for 25 min at room temperature with gentle agitation. Beads were washed an additional two times in buffer H/0.15 and kinetochores were then incubated in elution buffer (0.5 mg/mL 3Flag peptide in buffer H/0.15) for 30 min at room temperature with gentle agitation.

Quantification of the level of fluorescence after SDS-PAGE confirmed that the labeling reaction was specific, and that the amount of labeled protein in the eluate was maximized under these conditions (3). Laser trap assays confirmed that the fluorescent kinetochore particles were fully functional, forming attachments to growing microtubule tips with normal rupture strength.

Preparation of flow channels for fluorescent imaging

Glass coverslips and slides were cleaned in a benchtop plasma cleaner (model PDC-001, Harrick Plasma) for 5 min. Strips of double-sided tape (3M) were then laid onto each slide, perpendicular to the long edge of the slide, and coverslips were pressed onto the tape to create narrow channels, ~10 µL in volume. Before use, each assembly was warmed on a 60°C hot plate for 30 min and pressed again, to create a tighter seal between the double-sided tape, the coverslip, and the slide. Two or three channels were usually created side-by-side on a single slide, and small droplets of nail polish were added in-between the inlets and outlets to prevent fluids pipetted onto one channel from flowing into an adjacent channel.

To block non-specific binding of kinetochore particles, each flow channel was coated with a supported lipid bilayer prepared in the following manner. First, a lipid mixture including a small fraction (~0.1%) of biotinylated lipid was created by dissolving 300 µg of POPC (1-palmitoyl-2-oleoyl-*sn*-glycero-3-phosphocholine; Avanti Polar Lipids, Inc.) and 0.4 µg of biotinyl-cap-PE (1,2-dieoleoyl-*sn*-glycero-3-phosphoethanolamine-N-(cap biotinyl) sodium salt; Avanti) in ~100 µL of chloroform in a glass test tube. The lipid solution was thoroughly mixed, dried by flowing nitrogen over it for 5 min while simultaneously rotating the tube, and then desiccated in a vacuum chamber overnight. Dried lipid 'cakes' were stored for up to several weeks in a vacuum desiccator. A lipid cake was rehydrated by adding 300 µL BRB80 buffer (80 mM PIPES, 1 mM $MgCl_2$, 1 mM EGTA pH 6.9) and vortexing vigorously. Rehydrated lipids were then sonicated using a clean tip sonicator (model S450A, Branson) submerged directly into the sample for 5 min at 50% duty cycle and a low power setting. The initially cloudy lipid solution was clarified by the direct sonication, confirming that small unilamellar vesicles were created. Clarified lipids were used for up to several hours after the sonication. Each flow channel was pre-wetted with 10 µL of BRB80, coated by adding 10 µL of the clarified lipid mixture and incubating 4 min at room temperature, and then washed with 50 µL of BRB80.

Imaging of coverslip-tethered fluorescent kinetochore particles

Isolated kinetochore particles were tethered specifically to lipid-coated coverslip surfaces for viewing by fluorescence. First, 10 µL of 0.25 mg/mL streptavidin (Sigma-Aldrich) in BRB80 was introduced into a lipid-coated flow channel, incubated 4 min, and then washed with 50 µL BRB80. 10 µL of 20 µM biotinylated anti-Penta-His antibody (Qiagen) in BRB80 was then introduced, incubated 5 min, and washed in the same manner. Fluorescent kinetochore particles were diluted in BRB80 to a concentration corresponding to ~140 pM Dsn1, introduced into the channel, incubated 5 min, and then washed with 50 µL of BRB80 supplemented with 0.1 mg/mL κ-casein and an oxygen scavenging system (1 mM DTT, 250 µg/mL glucose oxidase, 30 µg/mL catalase, 25 mM glucose). The inlet and outlet of the channel were sealed, and individual kinetochores on the coverslip surface were viewed in a custom-built multi-color TIRF microscope with a computer-controlled 3-axis piezo specimen stage (4). An automated procedure was developed to rapidly record >200 images for each sample, using LabView software to raster the specimen stage while maintaining image focus. Using Mtw1-CLIP-647 as a fiducial marker, the concentration of kinetochore particles was adjusted to achieve surface densities between 50 and 300 particles per 1,500 μm^2 field of view. Individual bright spots were detected, and their brightness quantified by integrating over square, 7-by-7-pixel regions (0.28 μm^2 at the specimen) centered on the maxima. Additional details describing the image analysis are given below.

Imaging of fluorescent kinetochores attached laterally to microtubules

To view kinetochores attached laterally to microtubules, 10 µL of 0.25 mg/mL streptavidin (Sigma-Aldrich) in BRB80 was introduced into a lipid-coated channel, incubated 4 min, and then washed with 50 µL BRB80. 10 µL of 0.05 mg/mL biotinylated anti-α-tubulin antibody (BioLegend) was then introduced, incubated 5 min, and washed with 50 µL BRB80 plus 0.1 mg/mL κ-casein (BBC). 10 µL of Alexa-488-labeled, taxol-stabilized microtubules diluted in BBC were introduced, incubated 5 min, and washed with 50 µL BBC. Fluorescent kinetochore particles were then diluted in BBC to a concentration corresponding to ~140 pM Dsn1, introduced into the channel, incubated 5 min and then washed with BBC plus an oxygen scavenging system (described above). The inlet and outlet of the channel were sealed, and

individual kinetochores and microtubules were viewed in a custom, multi-color TIRF microscope, as described above.

Imaging of fluorescent kinetochores attached to the tips of microtubules

To view tip-attached kinetochores, fluorescent kinetochore particles were first tethered specifically to a lipid-coated coverslip as described above. Short, Alexa-488-labeled microtubules (5 to 10 μm in length) diluted in BBC were then introduced, incubated 5 min, and washed with 50 μL BBC. By thermal diffusion, the microtubules tended to attach to the kinetochores primarily by their ends. The inlet and outlet of the channel were sealed, and individual kinetochores and microtubules were viewed by multi-color TIRF microscopy. End-captured microtubules swiveled freely about their kinetochore-attached ends, occasionally also becoming attached via their sides to additional surface-tethered kinetochores. Surface-tethered kinetochores in the same fields of view that had not captured a microtubule served as internal controls.

Imaging of fluorescent kinetochores tracking with disassembling microtubule tips

To view kinetochores tracking processively with disassembling tips, dynamic microtubule extensions were first grown from coverslip anchored seeds. 10 μL of 0.25 mg/mL streptavidin (Sigma-Aldrich) in BRB80 was introduced into a lipid-coated channel, incubated 4 min, and then washed with 50 μL BRB80. 10 μL of biotinylated, GMPCPP-stabilized microtubule seeds in BRB80 were introduced, and incubated 5 min. 49 μL of microtubule growth buffer was prepared, consisting of 1.5 mg/mL fluorescent tubulin in BBC supplemented with 1 mM GTP and an oxygen scavenging system (described above). 1 μL of undiluted fluorescent kinetochore stock was then added, and the growth buffer was mixed and introduced into the flow channel. 10 min incubation at room temperature allowed fluorescent microtubule extensions to grow from the surface-anchored GMPCPP seeds and kinetochores to bind laterally to the extensions. Disassembly of the microtubules was then triggered by buffer exchange, introducing 15 μL BBC while simultaneously acquiring images by TIRF microscopy. All fluorescence imaging experiments were performed at room temperature.

Analysis of images of fluorescent kinetochores

For each image, we applied the method of (5) to find all local maxima separated by at least 7 pixels. Integrated brightness values were then computed by summing the intensities within square, 7-by-7-pixel regions (0.28 μm^2 at the specimen) surrounding every local maximum in both color channels. Histograms of these integrated brightness values showed a clear separation between the individual SNAP- and CLIP-dyes and the background fluorescence levels, allowing thresholds to be set for distinguishing dye-labeled particles from background noise. Individual kinetochore particles were identified by the presence of Mtw1-CLIP-647. After registration of the color channels (4), each kinetochore particle was classified as single-color, carrying only Mtw1-CLIP but lacking Mps1-SNAP-549, or dual-color, carrying both Mtw1 and Mps1. Colocalization was then calculated for each image by dividing the number of dual-color particles by the total number of particles. The distributions of integrated brightness values included sub-populations with just one detectable dye molecule, identifiable by their single-step photobleaching behavior, from which the unitary brightness for both Mps1-SNAP-549 and Mtw1-CLIP-647 was estimated (3). Ratios of Mps1 to Mtw1 molecules were then estimated for every particle by dividing their integrated brightness values in the 549-nm and 647-nm color channels by the corresponding unitary brightness and computing the ratio, Mps1-SNAP-549 to Mtw1-CLIP-647.

Kinase Assays

Kinetochores or Mps1 were purified and maintained on beads for kinase assays. After the purification, they were washed once in buffer H/0.15 without inhibitors and then incubated in kinase buffer (28 mM HEPES pH 8.0, 2.8 mM $MgCl_2$, 143 mM KCl, 14% glycerol, 0.1 mM EDTA, 0.5 mM EGTA, 0.1% NP-40, with or without 200 μM ATP) for the indicated period of time in a 30 °C water bath. The kinase buffer was made by diluting 10X kinase buffer (0.5 M HEPES pH 8.0, 0.1 M $MgCl_2$, 0.75 M KCl, 5% glycerol, 2 mM ATP) with buffer H/0.15. To assess release of endogenous Mps1, the supernatants were collected, and the bead-associated proteins were washed once in buffer H/0.15 with protease and phosphatase inhibitors prior to elution. Supernatants and bead-associated proteins were eluted by boiling in SDS sample buffer.

Bulk Binding Assays

To generate phosphorylated kinetochores lacking Mps1, a kinase reaction was performed with purified kinetochores maintained on beads. Mock reactions were also performed with beads generated from a mock IP with lysate lacking a Flag epitope-tagged protein. Next, the bead-associated proteins were washed twice in buffer H/0.15 without added inhibitors before going through subsequent treatments detailed below.

Assay to analyze the effect of kinetochore phosphorylation on Mps1 binding: Bead-associated kinetochores or mock-treated beads were incubated in buffer H/0.15 supplemented with 1mM $MnCl_2$ and 200 units of λ-phosphatase (NEB#PO753L) in a 30 °C water bath for 20 minutes. Mock phosphatase reactions also included phosphatase inhibitors (0.1 mM Na-orthovanadate, 0.2 μM microcystin, 2 mM β-glycerophosphate, 1 mM Na pyrophosphate, 5 mM NaF). Next, the beads were washed 3 times in buffer H/0.15 with protease and phosphatase inhibitors. Each reaction was then incubated with 1 ng of purified native Mps1-V5 in buffer H/0.15 with protease inhibitors and phosphatase inhibitors with gentle agitation at room temperature for 25 minutes. Following the binding reaction, bead-associated proteins were washed once in buffer H/0.15 with protease and phosphatase inhibitors and the proteins were eluted by boiling in SDS sample buffer.

Assay to analyze the effect of Mps1 autophosphorylation on kinetochore binding: All kinetochores or mock-treated beads were dephosphorylated by incubation in buffer H/0.15 supplemented with 1 mM $MnCl_2$ and 200 units of λ-phosphatase (NEB#PO753L) in a 30 °C water bath for 20 minutes. Next, bead-associated proteins were washed twice in buffer H/0.15 with protease and phosphatase inhibitors. Each reaction of bead-bound kinetochores or mock treated beads was then incubated with 5 ng native Mps1-V5 or 5 ng autophosphorylated P-Mps1-V5 in buffer H/0.15. After the binding reactions, the bead-associated proteins were washed once in buffer H/0.15 with protease and phosphatase inhibitors and the proteins were eluted by boiling in SDS sample buffer.

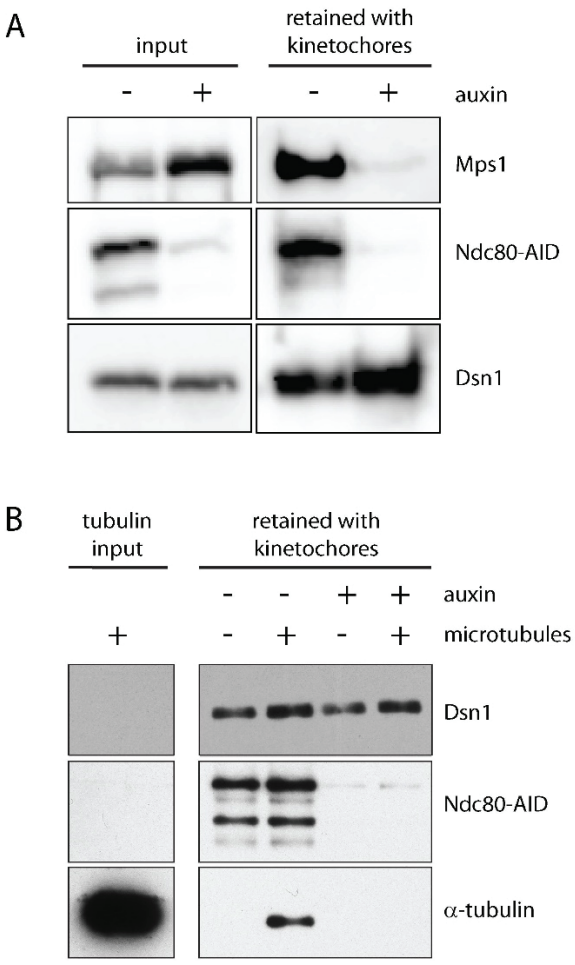

Supplementary Figure S1. Ndc80 is required for retention of Mps1 on purified kinetochores and for microtubule attachment. Yeast expressing Ndc80-AID (SBY12352) were grown to mid-log phase and then 500 μM of auxin (3-indoleacetic acid, IAA) or vehicle alone (DMSO) was added. Cells were harvested two hours later. (A) Kinetochores were bound to beads, washed, and then the levels of Mps1 and kinetochore proteins were assessed by SDS-PAGE followed by immunoblotting. (B) Kinetochores were bound to beads and either mock-treated or incubated with taxol-stabilized microtubules. The levels of kinetochore proteins and the amount of α-tubulin retained after washing the beads were then assessed by SDS-PAGE followed by immunoblotting.

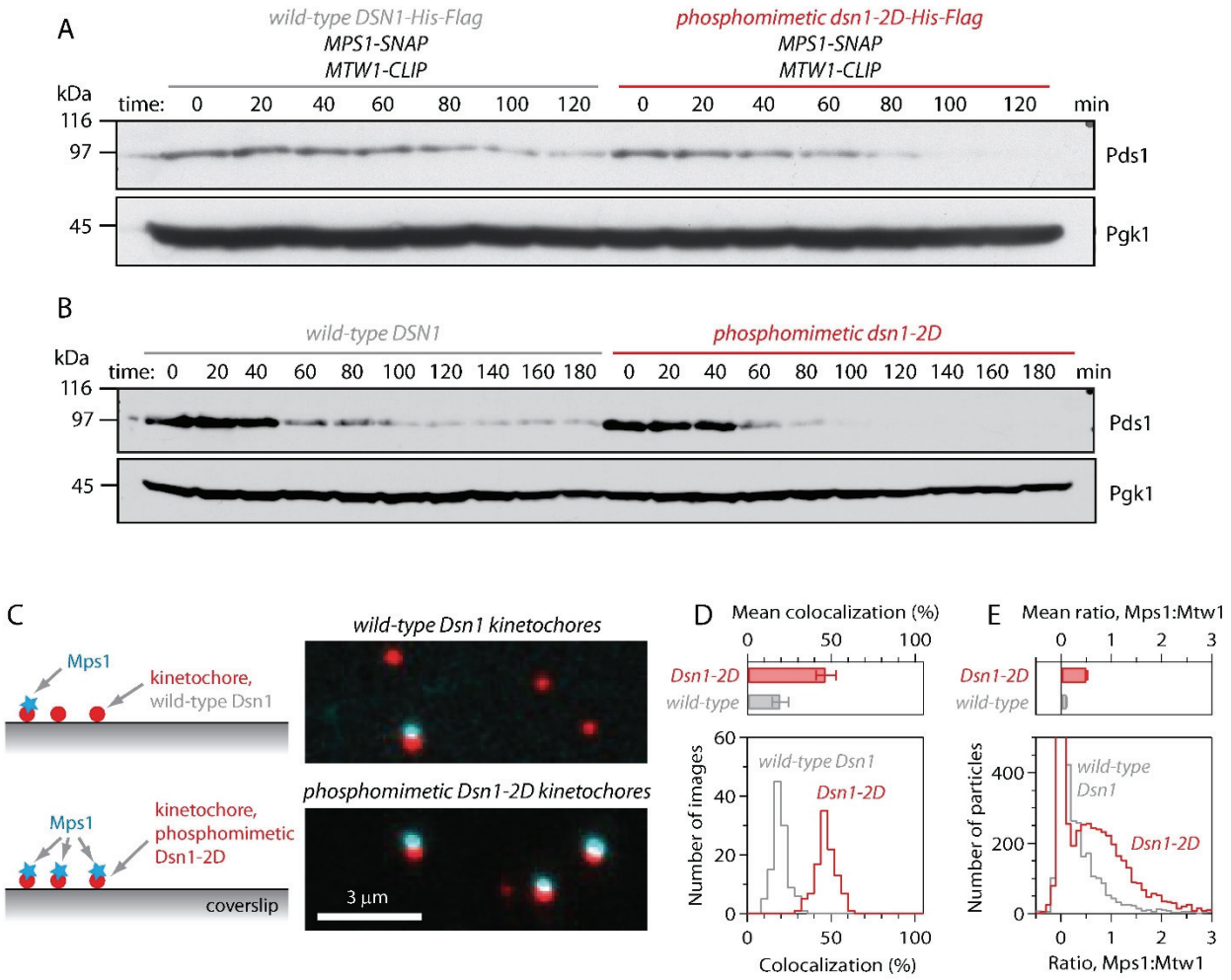

Supplementary Figure S2. Phosphomimetic Dsn1-2D improves retention of Mps1 on isolated kinetochores without disrupting checkpoint silencing in vivo. (A and B) *dsn1-2D* cells silence the spindle assembly checkpoint with wild-type-like kinetics. Yeast strains with wild-type Dsn1 or with phosphomimetic Dsn1-2D were arrested in prometaphase by exposure for 3 hours to the microtubule-depolymerizing drug, nocodazole. After nocodazole was washed out of the media, samples were collected at indicated timepoints and analyzed for levels of the anaphase inhibitor, Pds1 (securin), as well as a loading control, Pgk1 (phosphoglycerate kinase 1), by SDS-PAGE and immunoblotting. Sustained levels of Pds1 during nocodazole arrest indicate that the cells can generate robust checkpoint 'wait' signals. The drop in Pds1 levels 80 to 100 min after release from nocodazole indicates that the cells entered anaphase and therefore silenced the 'wait' signals. (A) Wild-type strain with *DSN1-His-Flag*, *MPS1-SNAP*, and *MTW1-CLIP* (SBY16381), versus phosphomimetic strain with *dsn1-2D-His-Flag*, *MPS1-SNAP*, and *MTW1-CLIP* (SBY16417). (B) Wild-type strain with *DSN1* (SBY4880), versus phosphomimetic strain with *dsn1-2D* (SBY8066). (C) Schematic diagram (left) and fluorescence images (right) of kinetochore particles carrying wild-type Dsn1 (top, from SBY12571) or phosphomimetic Dsn1-2D (bottom, from SBY15285). Both were labeled with Mps1-SNAP-549 (cyan) and Mtw1-CLIP-647 (red) and tethered to coverslips. Colors are offset vertically; cyan-red pairs are colocalized particles. (D) Percentages of kinetochore particles retaining Mps1. Bars show means (± SD) from N = 111 and 108 images of wild-type and Dsn1-2D particles, respectively. Histograms show corresponding distributions. (E) Approximate ratios of Mps1 to Mtw1 molecules, estimated from particle brightness relative to the brightness of single Mps1-SNAP-549 and Mtw1-CLIP-647 molecules. Bars show mean ratios (± SEM) from N = 8,863 and 6,891 wild-type and Dsn1-2D particles, respectively. Histograms show corresponding distributions.

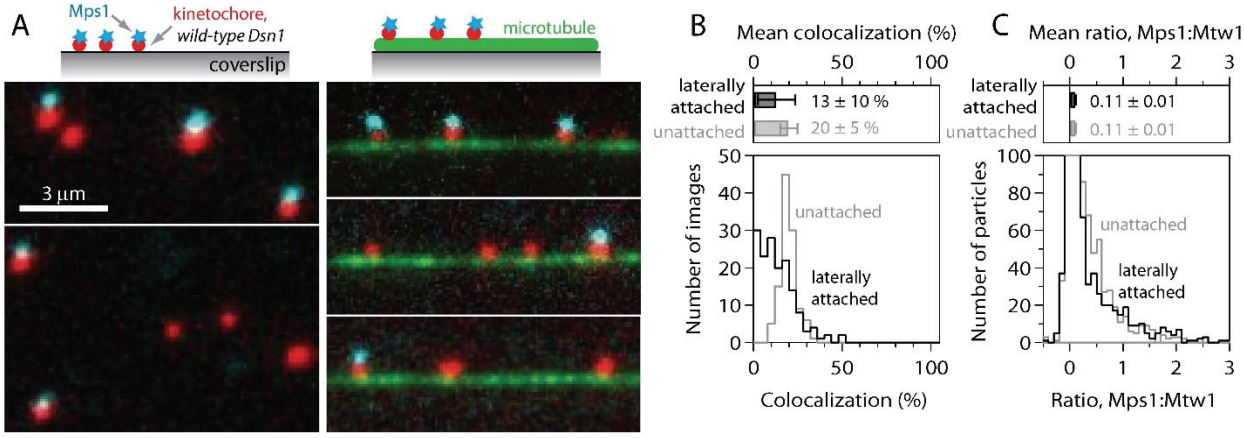

Supplementary Figure S3. Isolated wild-type kinetochores retain Mps1 when attached laterally to microtubules. (A) Fluorescence images of wild-type kinetochore particles (from SBY16381) carrying Mps1-SNAP-549 (cyan) and Mtw1-CLIP-647 (red), tethered to coverslips (left) or attached laterally to microtubules (green, right). Colors are offset vertically; cyan-red pairs are colocalized, dual-color particles. Fields containing multiple colocalized particles, as shown in the topmost images, were rare. (B) Percentages of wild-type kinetochore particles retaining Mps1. Bars show means (± SD) from N = 157 and 111 images of microtubule-attached and coverslip-tethered particles, respectively. Histograms show corresponding distributions. (C) Approximate ratios of Mps1 to Mtw1 molecules, estimated from particle brightness relative to the brightness of single Mps1-SNAP-549 and Mtw1-CLIP-647 molecules. Bars show mean ratios (± SEM) from N = 2,540 and 2,500 laterally attached and coverslip-tethered particles, respectively. Histograms show corresponding distributions.

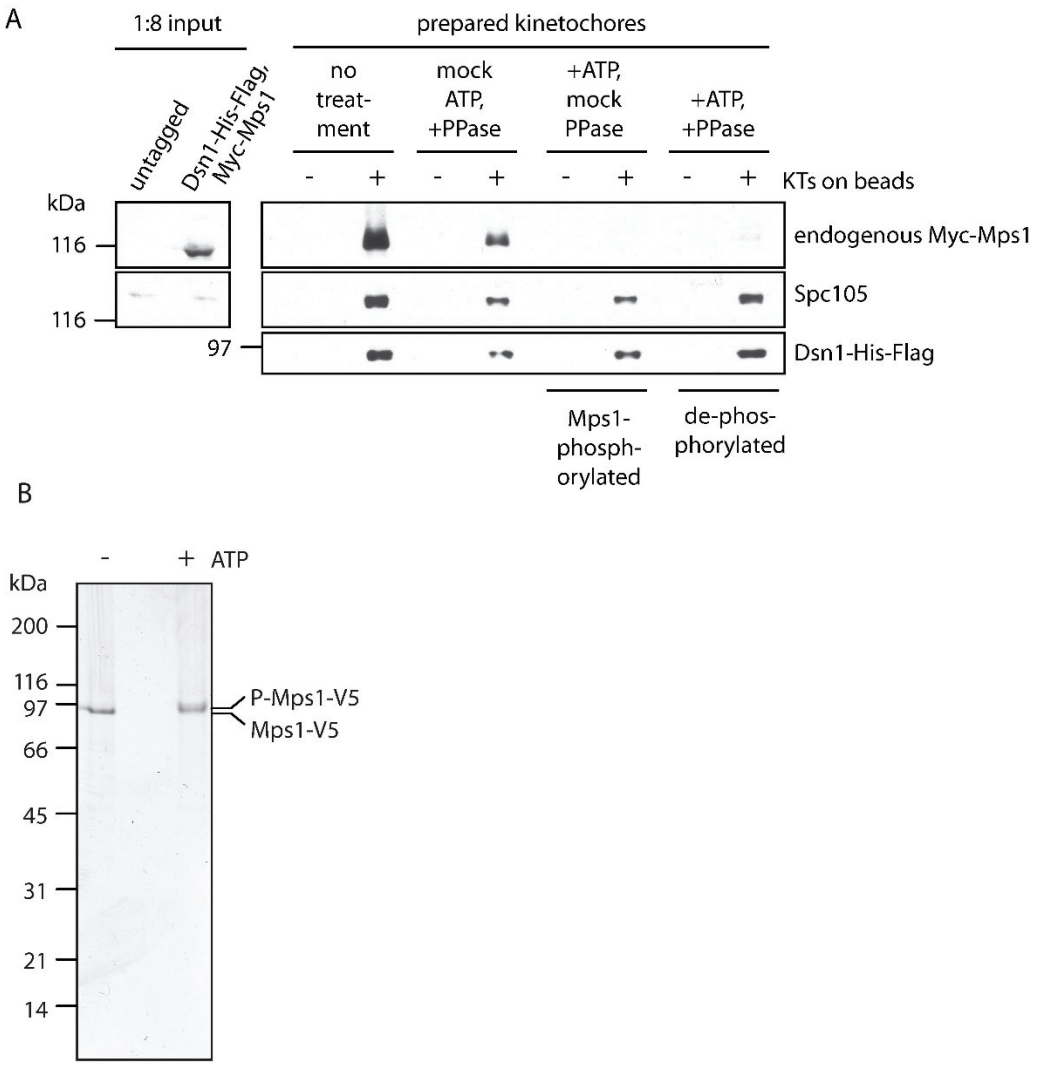

Supplementary Figure S4. Preparation of purified kinetochores and Mps1 for binding experiments. (A) Preparation of kinetochores phosphorylated by Mps1 or de-phosphorylated and lacking endogenous Mps1, for use in the experiment of Figure 4D. Kinetochores were purified (from SBY9190) via immunoprecipitation of Dsn1-His-Flag and maintained on beads. Control beads lacking kinetochores were also generated by immunoprecipitation from a wild-type strain lacking any tagged proteins (SBY3). Beads with or without kinetochores were incubated in kinase buffer with or without ATP. The ATP-treated samples were then divided and treated either with λ-phosphatase or with λ-phosphatase plus phosphatase inhibitors. All samples were analyzed by SDS-PAGE and immunoblotting. (B) Full-length Mps1 purified from budding yeast and induced to autophosphorylate by treatment with ATP. Mps1-V5 was purified (from SBY12412) via immunoprecipitation under stringent conditions to remove co-purifying proteins, incubated with or without ATP, and analyzed by silver-stained SDS-PAGE.

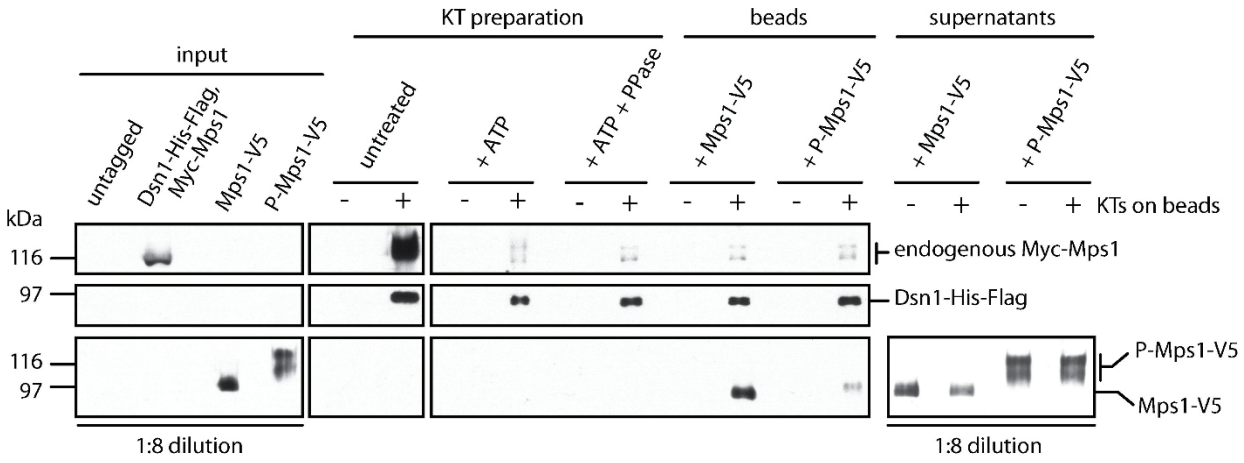

Supplementary Figure S5. Purified native Mps1, but not autophosphorylated Mps1, binds dephosphorylated kinetochores lacking endogenous Mps1. Kinetochores (KTs) were purified (from SBY9190) via immunoprecipitation of Dsn1-His-Flag and maintained on beads. Immunoprecipitation from a wild-type strain lacking any tagged proteins (SBY3) generated control beads lacking kinetochores. Immobilized kinetochores and control beads were incubated in kinase buffer with ATP to release endogenous Myc-Mps1 (+ATP), washed, and then dephosphorylated with λ-phosphatase (+ATP +PPase). Following phosphatase treatment, kinetochores or control beads were washed and incubated with either purified Mps1-V5 or autophosphorylated P-Mps1-V5 (prepared as in Figure 4B). All samples were analyzed by SDS-PAGE and immunoblotting. This figure shows results from the same experiment as in Figure 4E. Additional inputs and preparative steps are included here to illustrate the ATP-dependent release of endogenous Mps1 from kinetochores.

Supplementary Table S1. Yeast strains used in this study.

Strain	Genotype
SBY3	*Mat* a *ura3-1 leu2,3-112 his3-11 trp1-1 ade2-1 LYS2 can1-100 bar1*Δ
SBY3857	*Mat* a *ura3-1 leu2,3-112 his3-11 trp1-1 ade2-1 LYS2 can1-100 bar1-1 mps1::KAN::10Myc-MPS1:TRP1*
SBY4880	*Mat* a *ura3-1 leu2,3-112 his3-11 trp1-1 ade2-1 LYS2 can1-100 bar1-1 PDS1-18myc:LEU2*
SBY8066	*Mat* a *ura3-1 leu2,3-112 his3-11::DSN1-2D:HIS3 trp1-1 ade2-1 lys2*Δ *can1-100 bar1-1 PDS1-18myc:LEU2 dsn1::KANMX*
SBY9190	*Mat* a *ura3-1 leu2,3-112 his3-11 trp1-1 ade2-1 LYS2 can1-100 bar1-1 DSN1-6His-3Flag:URA3 mps1::KAN::10Myc-MPS1:TRP1*
SBY10327	*Mat* a *ura3-1 leu2,3-112 his3-11 trp1-1 ade2-1 LYS2 can1-100 bar1-1 DSN1-6His-3Flag:URA3 MTW1-CLIP:KanMX*
SBY12412	*Mat* a *ura3-1 leu2,3-112 his3-11 trp1-1 ade2-1 LYS2 can1-100 bar1-1 MPS1-3V5:KanMX*
SBY12352	*Mat* a *ura3-1 leu2,3-112 his3-11::pADH1-OsTIR1-myc:HIS3 trp1-1 DSN1-6His-3Flag:KanMx ade2-1 LYS2 can1-100 bar1-1 mps1::KanMx::10xmyc-MPS1::TRP1 Ndc80-3V5-IAA17:KanMX*
SBY12459	*Mat* alpha *ura3-1 leu2,3-112 his3-11 trp1-1 ade2-1 LYS2 can1-100 bar1-1 DSN1-6His-3Flag:URA3 MPS1-SNAP:HPH*
SBY12571	*Mat* a *ura3-1 leu2,3-112 his3-11 trp1-1 ade2-1 LYS2 can1-100 bar1-1 DSN1-6His-3Flag:URA3 MTW1-CLIP:KanMX MPS1-SNAP:HPH*
SBY15285	*Mat* a *ura3-1 leu2,3-112 his3-11 trp1-1 ade2-1 LYS2 can1-100 bar1-1 dsn1-2D-6His-3Flag:URA3 MTW1-CLIP:KanMX MPS1-SNAP:HPH*
SBY16381	*Mat* a *ura3-1, leu2,3-112 his3-11 trp1-1 ade2-1 LYS2 can1-100 bar1-1 DSN1-6His-3Flag:URA3 MTW1-CLIP:KanMX MPS1-SNAP:HPH PDS1-18myc:LEU2*
SBY16417	*Mat* a *ura3-1 leu2,3-112 his3-11 trp1-1 ade2-1 LYS2 can1-100 bar1-1 dsn1-2D-6His-3Flag:URA3 MTW1-CLIP:KanMX MPS1-SNAP:HPH PDS1-18myc:LEU2*

Supplementary Table S2. Plasmids used in this study.

Plasmid	Description	Source
pSB1821	*SNAP:HPH*	Aaron Hoskins, Moore Lab, U. Mass. Med.
pSB2067	*pFA6-3V5-IAA17:KANMX*	Leon Chan, Karsten Weis Lab, U.C. Berkeley
pSB2439	*dsn1-2D-6His-3Flag:URA3*	*this study*

Supplementary Table S3. Primers used in this study.

Primer	Description	Sequence (5' to 3')
SB654	*DSN1* forward primer at 200bp	GTGTCGAATTTGAGCCCCG
SB1510	*NDC80* C-terminal tagging forward	GGAAACGTCATTGAAGAGTTACGAAATTTGGAGTTTGAAACTGAACAT AACGTAACAAATcggatccccgggttaattaa
SB1511	*NDC80* C-terminal tagging reverse	CGGAAAGGTGGGGCTGAGCTTTGCTGTAGATTGCTCGGGTATTATAT ATCATTTATTTTAgaattcgagctcgtttaaac
SB2435	Reverse primer to amplify *DSN1-6His-3FLAG:URA3* from pSB2439	GTATATATAAATGTATGACTGTGTAATGTTACATATGCAGAAGTATCCG ATTTTTTTTTGATTTTTTCTTTTATTGATTCGGTAATCTCCGAACAG
SB4170	SNAP tagging C-terminus of *MPS1* forward	CAATGATGTGGTAGACACTGTTTTAAGGAAATTTGCAGATTACAAAATT GGT TCT GGT GGT TCT GGT atg gac aaa gac tgc gaa atg aag cgc ac
SB4171	SNAP tagging C-terminus of *MPS1* reverse	G TAT TTA TGT TCA TAA CTG GCA CAT GCT TTT CTT CCT TAT GCG GCT CTT gagctcgttttcgacactggatggc

Caption for Supplementary Movie S1. Kinetochores retain Mps1 when tracking with disassembling microtubule tips. A kinetochore particle (from SBY15285) tracks with the disassembling tip of a microtubule (green) while carrying Mps1-SNAP-549 (cyan) and Mtw1-CLIP-647 (red). Colors are deliberately offset; the cyan-red pair is a colocalized, dual-color kinetochore particle.

Supplementary References

1. Akiyoshi B*, et al.* (2010) Tension directly stabilizes reconstituted kinetochore-microtubule attachments. *Nature* 468(7323):576-579.

2. Miller MP, Asbury CL, & Biggins S (2016) A TOG Protein Confers Tension Sensitivity to Kinetochore-Microtubule Attachments. *Cell* 165(6):1428-1439.

3. Sarangapani KK*, et al.* (2014) Sister kinetochores are mechanically fused during meiosis I in yeast. *Science* 346(6206):248-251.

4. Deng Y & Asbury CL (2017) Simultaneous Manipulation and Super-Resolution Fluorescence Imaging of Individual Kinetochores Coupled to Microtubule Tips. *Methods Mol Biol* 1486:437-467.

5. Crocker JC & Grier DG (1996) Methods of digital video microscopy for colloidal studies. *J Colloid Interf Sci* 179(1):298-310.

6. Knop M*, et al.* (1999) Epitope tagging of yeast genes using a PCR-based strategy: more tags and improved practical routines. *Yeast* 15(10B):963-972.

7. Longtine MS*, et al.* (1998) Additional modules for versatile and economical PCR-based gene deletion and modification in Saccharomyces cerevisiae. *Yeast* 14(10):953-961.

8. Nishimura K, Fukagawa T, Takisawa H, Kakimoto T, & Kanemaki M (2009) An auxin-based degron system for the rapid depletion of proteins in nonplant cells. *Nat Meth* 6(12):917-922.

9. Shcherbakova I*, et al.* (2013) Alternative spliceosome assembly pathways revealed by single-molecule fluorescence microscopy. *Cell reports* 5(1):151-165.